Laboratori Nazionali di Frascati

Submitted to Nucl. Phys. B

LNF-93/017 (P)
30 Aprile 1993

M. Greco, A. Vicini:

PHOTOPRODUCTION OF HIGH P_T JETS IN NEXT-TO-LEADING ORDER QCD

PACS.: 13.87.Ca

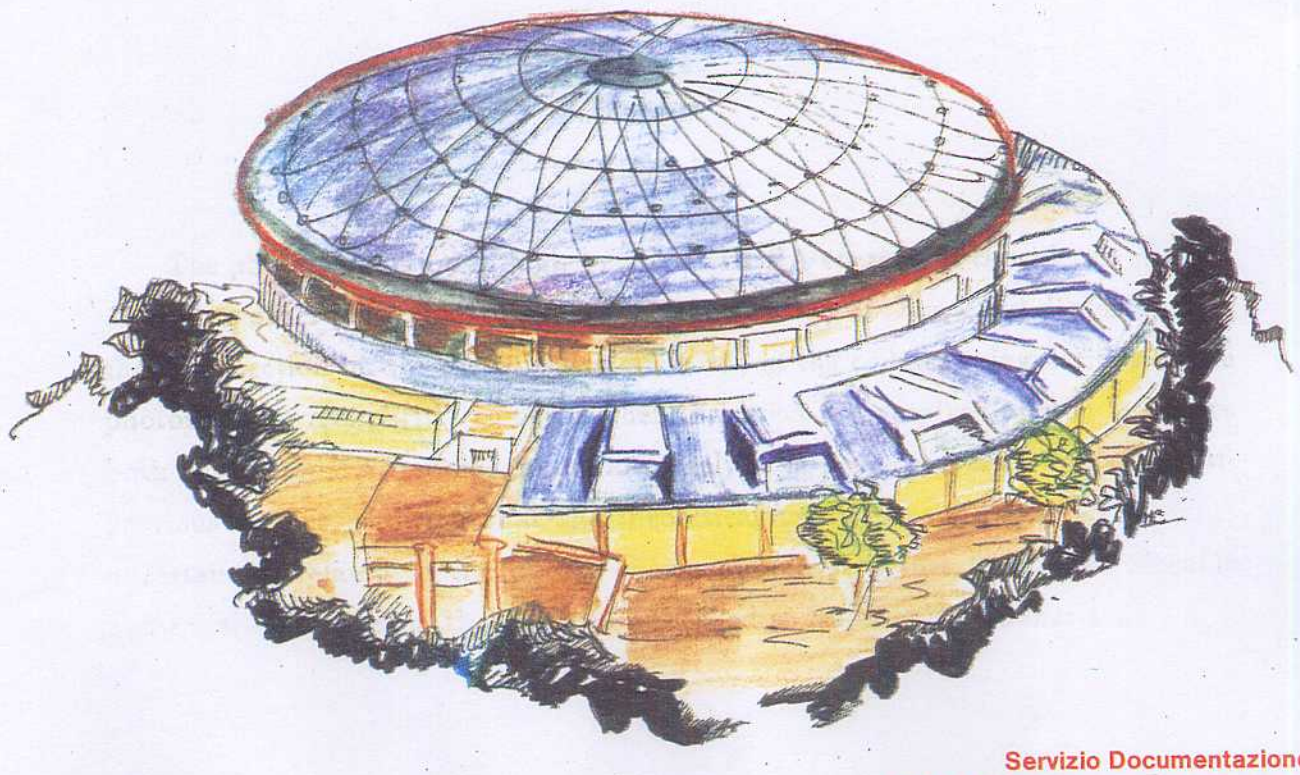

Servizio Documentazione
dei Laboratori Nazionali di Frascati
P.O. Box, 13 - 00044 Frascati (Italy)

INFN – Laboratori Nazionali di Frascati
Servizio Documentazione

LNF-93/017 (P)
30 Aprile 1993

PHOTOPRODUCTION OF HIGH P_T JETS IN NEXT-TO-LEADING ORDER QCD

M.Greco[a] and A.Vicini[b]

[a] *Dipartimento di Fisica Nucleare e Teorica, Università di Pavia, Italy*
INFN, Laboratori Nazionali di Frascati, Frascati, Italy
[b] *Dipartimento di Fisica, Università di Padova, Italy*
INFN, Sezione di Padova, Padova, Italy

Abstract

The photoproduction of high p_T jets at HERA energies is considered in next-to-leading order perturbative QCD. The cancellation of $O(\alpha_{em}\alpha_S^2)$ dependence of the cross section on the factorisation scale M_γ of the collinear singularities of the photon is shown explicitly to occur when the direct and resolved photon terms are both considered. A detailed numerical analysis is presented and compared with previous studies, showing that the theoretical predictions are affected by large uncertainties related to the poorly known photon structure functions. Sizeable numerical differences in the analyses published so far are also emphasized.

1.Introduction

The photoproduction of high p_T particles and jets at HERA will play an important role in testing QCD, providing a detailed source of information on the photon structure functions, particularly the gluon distribution, which are poorly determined at present. As well known [1], the photon contributes to the hard scattering with two distinct terms, namely with direct coupling to quarks and via its quark and gluon content (resolved photon). Both classes of terms are of order $\alpha_{em}\alpha_S$ and early calculations [2] of the Born cross sections indicated the dominance of the resolved part for $p_T < 40\ GeV$ and negative rapidities (the direction of the incoming electron defines $\eta_{lab} > 0$), suggesting a new possibility for studying the photon structure functions and particularly its gluonic contribution. First results on high p_T jets by the H1 and ZEUS collaborations have been presented very recently [3].

However, as it happened in the past in similar hard scattering studies [4,5], for a quantitative detailed jet cross section analysis one must go beyond the leading order (LO) QCD predictions, which are plagued by the usual theoretical uncertainties associated to the large scale dependence of $O(\alpha_{em}\alpha_S)$ terms. Indeed next-to-leading order (NLO) calculations of $O(\alpha_{em}\alpha_S^2)$ have been considered recently, first for the class of diagrams involving direct photons, showing [6,7] a reduced scale dependence of the one jet inclusive cross section at large p_T, as expected from similar results obtained in purely hadronic reactions beyond the leading order. However, unlike this latter case, the cross section $O(\alpha_{em}\alpha_S^2)$ still posseses a sizeable dependence on the factorisation scale M_γ of the collinear singularities of the photon at medium and small transverse momentum where, on the other hand, the resolved photon gives the dominant contribution. In addition, two further studies [7,8] have considered the role of NLO corrections for the resolved photon terms, exploiting the $O(\alpha_S^3)$ parton-parton scattering results of ref. [4], and using different LO and NLO parametrisations of the photon structure functions. Both analyses show a qualitative reduction of the scale dependence of the jet cross section, as clearly implied by the implementation of the Born terms with higher order

corrections.

In the present paper we perform a similar NLO analysis with a two-fold aim. First we explicitly show the cancellation of the dependence on the photon structure function factorisation scale M_γ to $O(\alpha_{em}\alpha_S^2)$, which occurs only when the direct and resolved photon terms are added up. Then we study in detail the dependence of the photoproduction cross section for the resolved photon term upon various parametrisations [9,10,11,12] of the photon structure functions, in particular those used in ref.[7,8]. Our results are not in complete agreement with the two previous analyses, particularly for what concerns the gluonic photon structure functions. It must be stressed that all the three results are based on the same $O(\alpha_S^3)$ parton-parton scattering calculation of ref.[4], implemented in an appropriate FORTRAN routine. We have carefully checked that our jet cross section does reproduce the previously published values for $p-\bar{p}$ collisions [4,13], when the photon and the anti-proton structure functions are appropriately interchanged. In order to disentangle the origin of the disagreement, several detailed distributions for the various parton subprocesses are presented. Finally we study the uncertainties which are present in the theoretical predictions, mainly coming from our poor knowledge of the photon structure functions, which hopefully will be reduced with the forthcoming experimental data.

The plan of the paper is the following. In sect.2 we present the general formalism and discuss the scale dependence of the jet cross-section. Numerical predictions for HERA experiments are displayed in sect.3 together with a discussion of the resulting theoretical uncertainty. Finally we give our conclusions in sect.4.

2.General formalism and scale dependence

The electron-proton jet cross section is obtained in the usual leading Weiszaecher-Williams equivalent photon approximation as

$$E\frac{d\sigma^{ep}}{d^3P} = 2\frac{\alpha_{em}}{\pi}\log\left(\frac{p_e\theta_{max}}{m_e}\right)\int_0^1 dx\frac{1+(1-x)^2}{2x}\,E\frac{d\sigma^{\gamma p}}{d^3P}(x) \qquad (1)$$

where p_e is the electron momentum. We will assume an angle cut $\theta_{max} = 5°$ for the scattered electron [14], $p_e = 30\ GeV$, $p_p = 820\ GeV$.

Let us consider first the resolved photon contribution, which has been shown [2] to play at HERA a dominant role at low p_T, namely $p_T < 40\ GeV$. Starting with the Sterman-Weinberg [15] definition of a jet in terms of a small angle δ, the jet photoproduction cross section can be written as

$$E\frac{d\sigma^{\gamma p}}{d^3P} = \frac{1}{\pi S}\sum_{i,j}\int_0^1 dx_1 \int_0^1 dx_2 F_i^p(x_1, M_p^2) F_j^\gamma(x_2, M_\gamma^2)\times$$
$$\times\left(\frac{\alpha_S(\mu^2)}{2\pi}\right)^2\left[\frac{1}{v}\sigma_{ij}^0(s,v)\delta(1-w) + \frac{\alpha_S(\mu^2)}{2\pi}K_{ij}(s,v,w;M_p^2,M_\gamma^2,\mu^2;\delta)\right] \quad (2)$$

where s, v and w are the partonic variables $s = x_1 x_2 S$, $v = \frac{x_2-1+V}{x_2}$, $w = \frac{x_2 VW}{x_1(x_2-1+V)}$ and $V = 1 + \frac{T}{S}$, $W = \frac{-U}{T+S}$, with S, T, U the hadronic Mandlestam variables. δ is the semiangle of the jet cone, σ_{ij}^0 are the partonic Born cross sections $O(\alpha_S^2)$, while K_{ij} are the finite higher order corrections $O(\alpha_S^3)$ [4]. We have kept distinct the factorisation mass scales of the proton and the photon structure functions. As usual, the latter are expressed in terms of the hadronic and the pointlike contributions as $F^\gamma(x,Q^2) = F_{had}^\gamma(x,Q^2) + F_{point}^\gamma(x,Q^2)$, and obey the appropriate evolution equation with the inhomogeneous term related to F_{point}^γ.

The partonic cross sections for one jet inclusive production have been calculated by Aversa et al.[4], starting from the squared matrix elements $O(\alpha_S^3)$ of Ellis et Sexton [16]. The initial state collinear divergences have been factorised and absorbed into the dressed structure functions in the $\overline{MS}$ scheme. Coherently with this choice, we have used for our numerical studies Morfin & Tung set B1 ($\Lambda_{QCD} = 194\ MeV$) [17] for the proton structure functions and three different parametrisations of the photon structure functions, namely the set of Aurenche et al. [11] to NLO (set I), that of Gordon and Storrow, also to NLO (set II) [9] and the set LAC1 of Abramowitcz et al. [10] to LO (set III). The last two have been used in the previous analyses [7,8]. In the next section we will show that the three photon sets can lead to sizeable differences in the kinematical range covered by the HERA experiments, inducing a quite large theoretical uncertainty in the

prediction of the jet cross sections. When completing the work presented here, a new NLO analysis of Kramer and Salesch [18] has come to our attention, where the set of photon structure functions of Glück et al.[12] has been used. We shall compare with these results whenever possible.

Most of our numerical results will be given with the jet definition described in ref.[19], as suggested in the Snowmass Accord [20], namely defining a jet as transverse energy deposited within a cone of radius R in the pseudorapidity azymuthal angle $(\eta - \phi)$ plane, with $R = 0.7$. To this aim we have followed the technique suggested in ref [13], namely implementing the analytical results of eq.(2) with a numerical integration of the $2 \rightarrow 3$ parton matrix elements in the region "$R - \delta$", with $\delta = 0.01$. The stability of our numerical results against changes in the assumed values od δ has been checked carefully.

Let us discuss now the dependence of the jet cross section on the various mass scales involved in eq.(2). As expected, the dependence on $\mu = M_p = M_\gamma = \xi p_T$ is very strong at the Born level, as shown in figs.(1) for $p_T = 5, 15, 50\ GeV$, for a jet configuration with $\eta_{lab} = -2$ and $R = 0.7$, for the various parametrisations of the photon structure functions. The effect is similar for sets I and II and larger for set III. The discontinuities in the slopes are simply due to CPU time limitation on the number of the theoretical data points. This is a general feature of all curves shown below. The introduction of NLO corrections reduces the scale dependence, as shown in the figures, similarly to what observed in the case of hadron-hadron collisions [4,5]. However, unlike the purely hadronic case, where the introduction of higher order terms reduces the sensitivity to renormalisation/factorisation mass scales to $O(\alpha_S^4)$, in case of photoproduction the presence of a pointlike component in the photon structure function induces a dependence to $O(\alpha_{em}\alpha_S^2)$ on M_γ^2, which is stronger at low p_T. This is shown in figs.(2-3), where we present the sensitivity of the jet cross section upon the photon and proton structure functions factorisation scales $\xi_\gamma = \frac{M_\gamma}{p_T}$ and $\xi_p = \frac{M_p}{p_T}$, for all the other scales fixed, at various p_T.

Indeed this dependence can be cancelled to $O(\alpha_{em}\alpha_S^2)$ only after summing up the direct and resolved photon NLO contributions, as shown in detail below.

In fact the splitting of the jet photoproduction into the direct and the resolved contributions induces this dependence explicitly in each term. In the case of the direct component this sensitivity was observed in refs. [6,7].

To simplify the discussion, defining symbolically the convolution product as $a \otimes b$, we can write the two contributions to the jet cross sections to NLO as:

$$\begin{aligned}
\left(E\frac{d\sigma}{d^3P}\right)_{dir} &= \frac{1}{\pi S}\frac{\alpha_{em}}{2\pi}\frac{\alpha_S(\mu^2)}{2\pi}\sum_i F_i^p(M^2)\otimes\left\{\sigma^0_{i\gamma\to jet+X}+\right. \\
&\qquad \left.+\frac{\alpha_S(\mu^2)}{2\pi}K(\mu^2,M^2,M_\gamma^2,\delta)_{i\gamma\to jet+X}\right\}, \\
\left(E\frac{d\sigma}{d^3P}\right)_{res} &= \frac{1}{\pi S}\left(\frac{\alpha_S(\mu^2)}{2\pi}\right)^2\sum_{i,j} F_i^p(M^2)F_j^\gamma(M_\gamma^2)\otimes\otimes\left\{\bar\sigma^0_{ij\to jet+X}+\right. \\
&\qquad \left.+\frac{\alpha_S(\mu^2)}{2\pi}\overline{K}(\mu^2,M^2,M_\gamma^2,\delta)_{ij\to jet+X}\right\},
\end{aligned} \tag{3}$$

with obvious meaning for the K and $\overline{K}$ functions. Defining $t=\log\left(\frac{M_\gamma^2}{\Lambda^2}\right)$, we have

$$\frac{\partial}{\partial t}\left(E\frac{d\sigma}{d^3P}\right)_{dir} = \frac{1}{\pi S}\frac{\alpha_{em}}{2\pi}\left(\frac{\alpha_S(\mu^2)}{2\pi}\right)^2\sum_i F_i^p(M^2)\otimes\frac{\partial}{\partial t}K_{i\gamma} \tag{4a}$$

$$\begin{aligned}
\frac{\partial}{\partial t}\left(E\frac{d\sigma}{d^3P}\right)_{res} &= \frac{1}{\pi S}\left(\frac{\alpha_S(\mu^2)}{2\pi}\right)^2\left\{\sum_{i,j}F_i^p(M^2)\left[\frac{\alpha_{em}}{2\pi}P_{\gamma j}+\frac{\alpha_S}{2\pi}\sum_k F_k^\gamma\otimes P_{jk}\right]\right. \\
&\qquad \left.\otimes\otimes\left[\bar\sigma^0_{ij\to jet+X}+\frac{\alpha_S}{2\pi}\overline{K}_{ij}\right]+\frac{\alpha_S}{2\pi}\sum_{i,j}F_i^pF_j^\gamma\otimes\otimes\frac{\partial}{\partial t}\overline{K}_{ij}\right\}
\end{aligned} \tag{4b}$$

where the eq.(4b) follows from the evolution equation of the photon structure function.

Due to initial state collinear divergences the dependence of $K_{i\gamma}$ on M_γ^2 is of the form

$$K(\mu^2,M^2,M_\gamma^2,\delta)_{i\gamma}=\sum_k P_{\gamma k}\otimes\bar\sigma^0_{ik}\log\left(\frac{\Lambda^2}{M_\gamma^2}\right)+K(\mu^2,M^2,\Lambda^2,\delta)_{i\gamma}$$

and therefore, adding the two terms in eqs.(4), the $O(\alpha_{em}\alpha_S^2)$ dependence on M_γ^2 is exactly cancelled. (*)

(*) A similar result is found in ref.[11] for the photoproduction of direct photon.

This concludes the discussion on the mass scales sensitivity of the jet cross section.

3.Results and discussion

We present here various numerical results for the three sets of photon strcture functions, studying in particular the uncertainties of the theoretical predictions. We will not report explicitly the effect of the variation of the proton structure functions, the resulting theoretical uncertainty being much smaller than what found for the photon case.

In order to show the general p_T behaviour of the jet cross section, as well as the various parton-parton scattering contributions, $\frac{d\sigma}{d\eta dp_T}$ is plotted in fig. (4) for $R = 0.7, \eta_{lab} = -2$ (near the maximum of the rapidity distribution), $\mu = M_p = M_\gamma = p_T$, and for set I. In Table I we give for comparaison the numerical results of the p_T distribution for the three sets of structure functions. Then in fig (5) we show the rapidity distribution, for $p_T = 15\ GeV$, $R = 0.7$ and $\mu = M_p = M_\gamma = p_T$, for the three sets of structure functions. The different behaviour between set III and sets I and II is more explicitly displayed in Table II, where we observe differences up to about 50%, particularly at large and negative η_{lab}. This result is mostly related to the small x behaviour of the gluon distribution of the photon, which is particularly steep for the set III. More in detail at the parton level, figs.(6a,b,c,d) show that the disagreement is higher when the gluonic content of the photon is compared for the three sets. On the other hand, the differences between sets I and II do not exceed a (10-20)% level.

The cone size dependence is shown in fig.(7), together with the Born terms, again for $p_T = 15\ GeV$, $\eta_{lab} = -2$, $\mu = M_p = M_\gamma = p_T$, for the three different sets. For comparaison we have also plotted our results with the set of structure functions of Glück, Reya and Vogt [12], defined as set IV, used in ref.[18]. (*) In spite of the different size of the Born level, the slope is similar for the four sets.

(*) Set IV is given in the DIS factorisation scheme. Coherently with this choice we use the Morfin & Tung set B1 [17] in the same factorisation scheme.

However fig.(7) has to be compared with fig.(4.b) of ref.[18], where a Born cross section of about 250 pb/GeV and $\sigma_{NLO} = \sigma_{Born}$ for $R \approx 0.7$ are found. It should be stressed also that our result with set II does not agree completely with that published by Gordon and Storrow [7]. Indeed in ref.[7] a Born cross section is found of about 200 pb/GeV at $p_T = 15\ GeV$, $\eta_{lab} = -2$, about 40% higher than what shown in fig 7 with set II.

At the light of the above results, in poor agreement with refs.[7,8,18], we have accurately checked our numerical analyses. In particular we have been able to reproduce with very good accuracy the proton- antiproton jet results previously published [4,13], when the photon and antiproton structure functions are appropriately interchanged, as already stated above. For the purpose of future comparaison, we give in Table III the results of jet cross sections in γp collisions, for $\mu = M_p = M_\gamma = p_T = 15\ GeV$, $\eta_{lab} = -2$, $p_\gamma = 30\ GeV$, $p_p = 820\ GeV$ at the Born level and NLO for $R = 0.7$. We stress the fact that the differences from the various sets of structure functions is much more enhanced for the γp cross section with respect to the ep results. Finally we show in fig.(8) the inclusive jet cross section, integrated on the rapidity, for low p_T values, which is of immediate phenomenological interest for HERA experiments. The direct photon contribution is one order of magnitude smaller.

4.Conclusions

A complete next-to-leading order calculation of inclusive one jet production in electron-proton collisions has been presented, particularly via the resolved photon mechanism. We have discussed in detail the scale dependence of the NLO results, showing explicitly that a complete cancellation of the $O(\alpha_{em}\alpha_S^2)$ scale dependence occurs only upon addition of the direct and resolved photon contributions. Furthermore we have studied carefully the effects of the theoretical uncertainties related to our poor knowledge of the photon strcture functions, pointing out in particular that the various analyses existing so far disagree by factors of order one at the level of γp cross section. More work from all groups is needed, to control

the accuracy of the numerical calculations. To this aim we have given detailed partial results for the various parton processes contributing to the photon proton jet cross section.

From the results of the present analysis, it seems to us quite premature that current experiments can provide soon information on the gluon distribution functions of the photon. On the other hand the quark content of the photon could be more easily disentangled at reasonably small p_T.

We would like to thank J.Ph. Guillet for continuous advice in the numerical analysis and discussions. We are also grateful to M. Fontannaz for providing us with the FORTRAN code of the photon structure functions of ref.[11] prior to publication.

References

[1] E.Witten, Nucl.Phys. B120 (1977) 189.

[2] M.Drees and R.M.Godbole, Phys.Rev.D39 (1989) 169;
H.Baer, J.Ohnemus and J.F.Owens, Z.Phys.C42 (1989) 657.

[3] H1 Collaboration, T.Ahmed et al., Phys.Lett. B297 (1992) 205;
ZEUS Collaboration, M.Derrick et al., DESY 92-138 (1992).
See also C.Berger and R.Nania, invited talks to "Rencontres de Physique de la Vallée d'Aoste", La Thuile, March 1993.

[4] F.Aversa, P.Chiappetta, M.Greco and J.Ph.Guillet, Nucl.Phys.B327 (1989) 105.

[5] R.K.Ellis,P.Nason and S.Dawson, Nucl.Phys.B303 (1988) 724;
W.Beenaker, H.Kuijf,W.L.Van Neerven and J.Smith, Phys.Rev.D40 (1989) 54.

[6] D.Boedeker, proc. of "Physics at HERA" Workshop, Hamburg 1991, vol.1,657 edit. W.Büchmuller and G.Ingelman;
DESY preprint, DESY 92-059 (1992).

[7] L.E.Gordon and J.K.Storrow, Phys.Lett.B291 (1992) 320.

[8] G.Kramer and S.G.Salesch, proc. "Physics at HERA" Workshop, Hamburg 1991, vol.1,649, edit. W.Büchmuller and G.Ingelman.

[9] L.E.Gordon and J.K.Storrow Manchester preprint M/C.TH.91/29 (1991).

[10] H.Abramowicz, A.Levy and K.Charchula, Phys.Lett.B269 (1991) 458.

[11] P.Aurenche, P.Chiappetta, M.Fontannaz, J.Ph.Guillet and E.Pilon, Orsay preprint, LPTHE Orsay 92/13 (1992).

[12] M.Glück, E.Reya and A.Vogt, Phys.Rev. D45 (1992) 3986; Phys.Rev. D46 (1992) 1973.

[13] F.Aversa, P.Chiappetta, L.Gonzales, M.Greco and J.Ph.Guillet, Z.Phys.C49 (1991) 459.

[14] H.Baer et al., ref.[2].

[15] G.Sterman and S.Weinberg, Phys.Rev.Lett.39 (1977) 1436.

[16] R.K.Ellis and J.C.Sexton, Nucl.Phys.B269 (1986) 445.

[17] J.G.Morfin and Wu-Ki Tung, Z.Phys.C52 (1991) 13.

[18] G.Kramer and S.G.Salesch, DESY preprint DESY 93-010 (1993).

[19] S.D.Ellis, Z.Kunszt and D.E.Soper, Phys.Rev.D40 (1989) 2188.

[20] J.E.Huth et al., FERMILAB-Conf-90/249-E (1990).

$d\sigma^{(ep)}/d\eta dp_T$ (pb/GeV)						
p_T	set I		set II		set III	
	Born	NLO	Born	NLO	Born	NLO
5	$3.28\ 10^4$	$3.07\ 10^4$	$2.67\ 10^4$	$2.61\ 10^4$	$8.64\ 10^4$	$8.27\ 10^4$
8	$3.81\ 10^3$	$3.49\ 10^3$	$3.09\ 10^3$	$2.92\ 10^3$	$6.46\ 10^3$	$6.17\ 10^3$
10	$1.30\ 10^3$	$1.17\ 10^3$	$1.14\ 10^3$	$1.06\ 10^3$	$1.83\ 10^3$	$1.69\ 10^3$
12	521	477	449	422	647	597
14	231	211	199	187	265	238
15	160	142	139	129	177	161
20	34.0	31.3	29.8	29.7	33.6	31.0
25	9.48	8.90	8.53	8.17	8.85	8.34
30	3.14	2.96	2.85	2.69	2.85	2.77
35	1.20	1.14	1.07	1.12	1.07	1.01
40	0.50	0.47	0.43	0.45	0.44	0.41

TABLE I – p_T distribution $\frac{d\sigma^{(ep)}}{d\eta\, dp_T}$ for R = 0.7, $\eta_{lab} = -2$, $\mu = M_p = M_\gamma = p_T$. The results for sets I, II and III of photon structure functions are compared.

$d\sigma^{(ep)}/d\eta dp_T$ (pb/GeV)						
η_{lab}	set I		set II		set III	
	Born	NLO	Born	NLO	Born	NLO
-4.5	0.09	0.027	0.078	0.035	0.10	-0.01
-4	11.2	8.10	9.80	8.00	15.8	11.8
-3.5	44.4	38.5	38.8	36.9	61.9	59.1
-3	88.1	81.1	76.9	77.3	114	110
-2.5	131	121	114	111	157	145
-2	160	144	139	129	177	159
-1.5	181	158	157	145	183	160
-1	177	154	155	138	170	146
-0.5	161	143	141	128	150	132
0	140	126	121	108	129	112
0.5	115	100	92.0	80.0	100	86.0
1	63.6	52.8	46.4	37.5	49.8	40.0

TABLE II – η_{lab} = distribution $\frac{d\sigma^{(ep)}}{d\eta\, dp_T}$ for R = 0.7, p_T = 15 GeV, $\mu = M_p = M_\gamma = p_T$. The results for sets I, II and III of photon structure functions are compared.

TABLES III – η_{lab} = distribution $\frac{d\sigma^{(\gamma p)}}{d\eta\, dp_T}$ for $\sqrt{s_{\gamma p}}$ = 314 GeV, R = 0.7, p_T = 15 GeV, $\mu = M_p = M_\gamma = p_T$. The results for the different parton–parton subprocesses and sets I, II and III are displayed.

$d\sigma^{(\gamma p)}/d\eta dp_T$ (pb/GeV) set I								
η_{lab}	$qq \rightarrow jet + X$		$q(\gamma)g(p) \rightarrow jet + X$		$q(p)g(\gamma) \rightarrow jet + X$		$gg \rightarrow jet + X$	
	Born	NLO	Born	NLO	Born	NLO	Born	NLO
-4.5	2.53	-0.33	0.08	0.051	1.74	0.77	0.051	0.054
-4	183	58.6	41.5	20.6	190	165	36.8	35.7
-3.5	541	437	352	288	583	552	312	300
-3	846	751	$1.08\ 10^3$	$1.00\ 10^3$	867	827	902	861
-2.5	$1.08\ 10^3$	$1.05\ 10^3$	$2.12\ 10^3$	$1.69\ 10^3$	$1.02\ 10^3$	926	$1.59\ 10^3$	$1.43\ 10^3$
-2	$1.26\ 10^3$	$1.20\ 10^3$	$3.25\ 10^3$	$2.88\ 10^3$	$1.08\ 10^3$	$1.02\ 10^3$	$2.15\ 10^3$	$1.95\ 10^3$
-1.5	$1.38\ 10^3$	$1.29\ 10^3$	$4.25\ 10^3$	$3.32\ 10^3$	$1.06\ 10^3$	995	$2.46\ 10^3$	$2.12\ 10^3$
-1	$1.45\ 10^3$	$1.35\ 10^3$	$5.04\ 10^3$	$4.36\ 10^3$	972	867	$2.48\ 10^3$	$2.27\ 10^3$
-0.5	$1.50\ 10^3$	$1.44\ 10^3$	$5.62\ 10^3$	$5.03\ 10^3$	813	706	$2.21\ 10^3$	$2.06\ 10^3$
0	$1.58\ 10^3$	$1.45\ 10^3$	$6.11\ 10^3$	$5.41\ 10^3$	587	458	$1.67\ 10^3$	$1.54\ 10^3$
0.5	$1.80\ 10^3$	$1.62\ 10^3$	$6.99\ 10^3$	$6.32\ 10^3$	322	242	942	895
1	$2.54\ 10^3$	$2.31\ 10^3$	$9.18\ 10^3$	$8.43\ 10^3$	94.1	85.3	266	212

TABLE IIIa

$d\sigma^{(\gamma p)}/d\eta dp_T$ (pb/GeV) set II								
η_{lab}	$qq \rightarrow jet + X$		$q(\gamma)g(p) \rightarrow jet + X$		$q(p)g(\gamma) \rightarrow jet + X$		$gg \rightarrow jet + X$	
	Born	NLO	Born	NLO	Born	NLO	Born	NLO
-4.5	2.12	0.24	0.071	0.051	1.53	0.73	0.044	0.041
-4	155	72.8	35.5	21.6	166	147	31.4	31.9
-3.5	456	388	301	273	507	488	275	271
-3	717	666	932	876	756	728	798	750
-2.5	923	933	$1.83\ 10^3$	$1.58\ 10^3$	896	851	$1.42\ 10^3$	$1.29\ 10^3$
-2	$1.08\ 10^3$	$1.04\ 10^3$	$2.80\ 10^3$	$2.29\ 10^3$	958	818	$1.94\ 10^3$	$1.82\ 10^3$
-1.5	$1.18\ 10^3$	$1.06\ 10^3$	$3.67\ 10^3$	$3.87\ 10^3$	957	847	$2.24\ 10^3$	$1.92\ 10^3$
-1	$1.25\ 10^3$	$1.25\ 10^3$	$4.37\ 10^3$	$3.88\ 10^3$	896	804	$2.29\ 10^3$	$2.11\ 10^3$
-0.5	$1.32\ 10^3$	$1.29\ 10^3$	$4.90\ 10^3$	$4.60\ 10^3$	761	657	$2.06\ 10^3$	$1.95\ 10^3$
0	$1.42\ 10^3$	$1.34\ 10^3$	$5.40\ 10^3$	$5.12\ 10^3$	552	427	$1.56\ 10^3$	$1.42\ 10^3$
0.5	$1.64\ 10^3$	$1.46\ 10^3$	$6.18\ 10^3$	$5.56\ 10^3$	297	218	855	814
1	$2.13\ 10^3$	$2.03\ 10^3$	$7.39\ 10^3$	$6.83\ 10^3$	73.1	67.8	201	162

TABLE IIIb

$d\sigma^{(\gamma p)}/d\eta dp_T$ (pb/GeV) set III								
η_{lab}	$qq \rightarrow jet + X$		$q(\gamma)g(p) \rightarrow jet + X$		$q(p)g(\gamma) \rightarrow jet + X$		$gg \rightarrow jet + X$	
	Born	NLO	Born	NLO	Born	NLO	Born	NLO
-4.5	2.53	0.31	0.083	0.058	3.15	1.36	0.085	0.088
-4	204	96.7	44.1	27.6	535	442	93.0	90.9
-3.5	608	498	377	322	$1.69\ 10^3$	$1.54\ 10^3$	814	795
-3	930	858	$1.14\ 10^3$	986	$2.39\ 10^3$	$2.21\ 10^3$	$2.18\ 10^3$	$2.05\ 10^3$
-2.5	$1.16\ 10^3$	$1.08\ 10^3$	$2.17\ 10^3$	$2.09\ 10^3$	$2.57\ 10^3$	$2.39\ 10^3$	$3.44\ 10^3$	$3.44\ 10^3$
-2	$1.30\ 10^3$	$1.22\ 10^3$	$3.24\ 10^3$	$2.68\ 10^3$	$2.37\ 10^3$	$2.22\ 10^3$	$3.99\ 10^3$	$3.93\ 10^3$
-1.5	$1.37\ 10^3$	$1.14\ 10^3$	$4.16\ 10^3$	$3.82\ 10^3$	$1.88\ 10^3$	$1.73\ 10^3$	$3.73\ 10^3$	$3.54\ 10^3$
-1	$1.40\ 10^3$	$1.33\ 10^3$	$4.86\ 10^3$	$4.03\ 10^3$	$1.26\ 10^3$	$1.10\ 10^3$	$2.88\ 10^3$	$2.52\ 10^3$
-0.5	$1.45\ 10^3$	$1.42\ 10^3$	$5.41\ 10^3$	$4.88\ 10^3$	733	639	$1.93\ 10^3$	$1.77\ 10^3$
0	$1.59\ 10^3$	$1.42\ 10^3$	$6.03\ 10^3$	$5.40\ 10^3$	419	326	$1.24\ 10^3$	$1.12\ 10^3$
0.5	$1.87\ 10^3$	$1.75\ 10^3$	$6.70\ 10^3$	$6.29\ 10^3$	239	186	742	680
1	$2.26\ 10^3$	$1.99\ 10^3$	$7.79\ 10^3$	$6.80\ 10^3$	77.0	67.8	226	213

TABLE IIIc

FIGS. 1 – Dependence of $\frac{d\sigma^{(ep)}}{d\eta\, dp_T}$ on the renormalisation/factorisation mass scales, for = 0.7, $\eta_{lab} = -2$, $\mu = M_p = M_\gamma = \xi p_T$ and for different values of p_T: $p_T = 5$ GeV (Fig. 1a); $p_T = 15$ GeV (Fig. 1b); $p_T = 50$ GeV (Fig. 1c). The results for sets I, II and III (see text) of photon structure functions are compared.

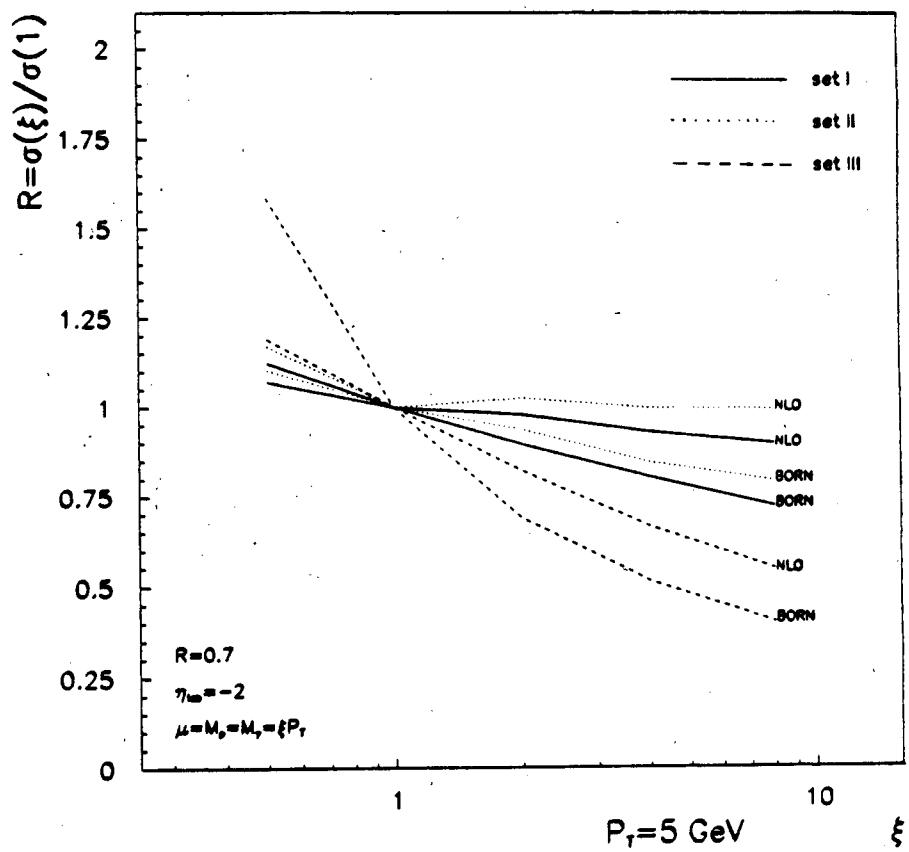

FIG. 1a

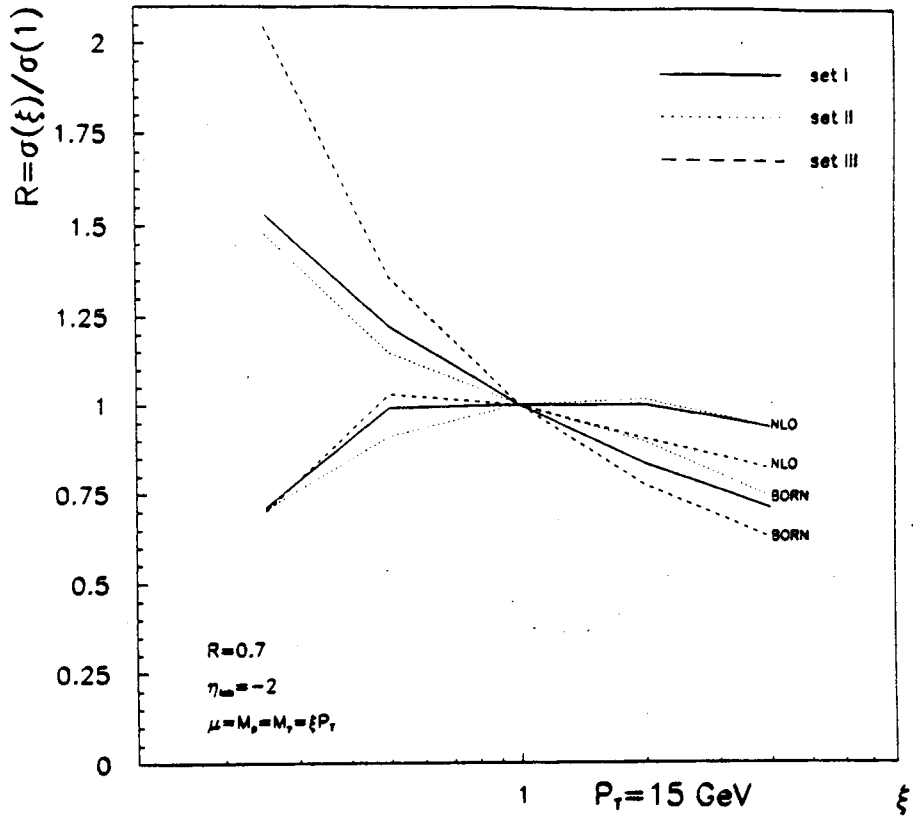
R=σ(ξ)/σ(1)
2
1.75
1.5
1.25
1
0.75
0.5
0.25
0
set I
set II
set III
NLO
NLO
BORN
BORN
R=0.7
$\eta_{jet}=-2$
$\mu=M_p=M_T=\xi P_T$
1
P_T=15 GeV
ξ

FIG. 1b

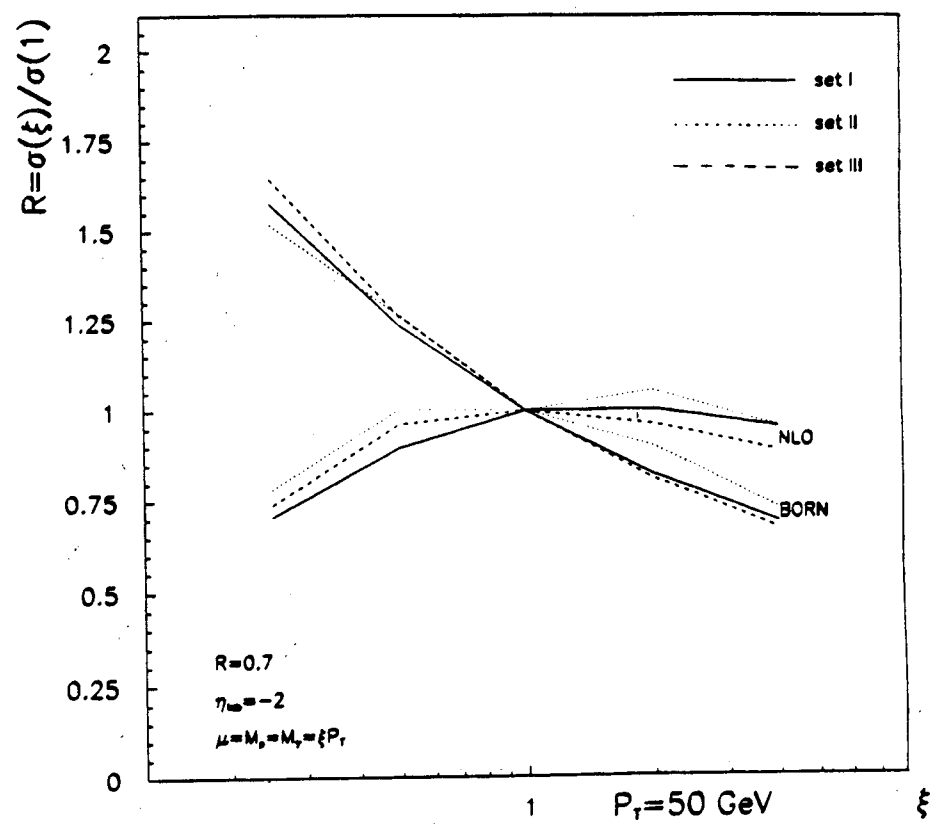
R=σ(ξ)/σ(1)
2
1.75
1.5
1.25
1
0.75
0.5
0.25
0
set I
set II
set III
NLO
BORN
R=0.7
$\eta_{jet}=-2$
$\mu=M_p=M_T=\xi P_T$
1
P_T=50 GeV
ξ

FIG. 1c

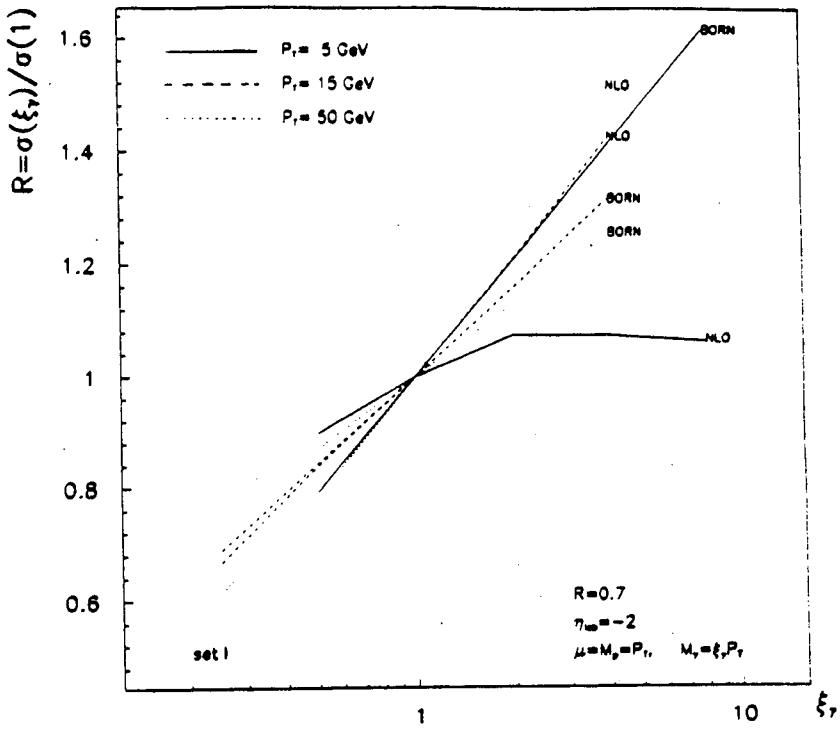

FIG. 2 – Dependence of $\frac{d\sigma^{(ep)}}{d\eta\, dp_T}$ on the photon factorisation scale M_γ for R = 0.7, $\eta_{lab} = -2$, $\mu = M_p = p_T$, $M_\gamma = \xi_\gamma p_T$ and for different values of p_T. Set I has been used for the photon structure functions.

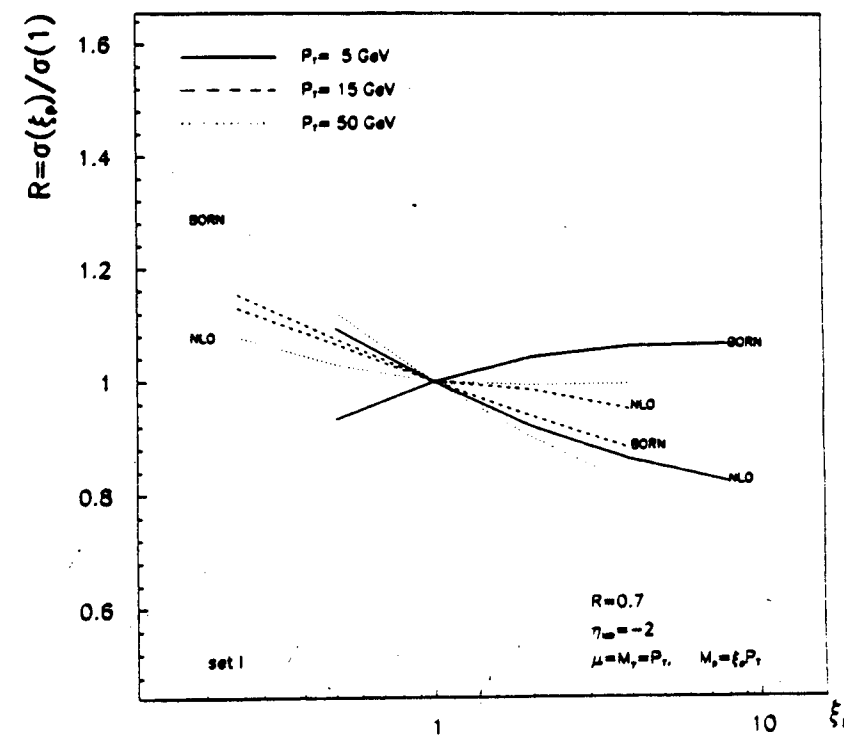

FIG. 3 – Dependence of $\frac{d\sigma^{(ep)}}{d\eta\, dp_T}$ on the proton factorisation scale M_p for R = 0.7, $\eta_{lab} = -2$, $\mu = M_\gamma = p_T$, $M_p = \xi_p p_T$ and for different values of p_T. Set I has been used for the photon structure functions.

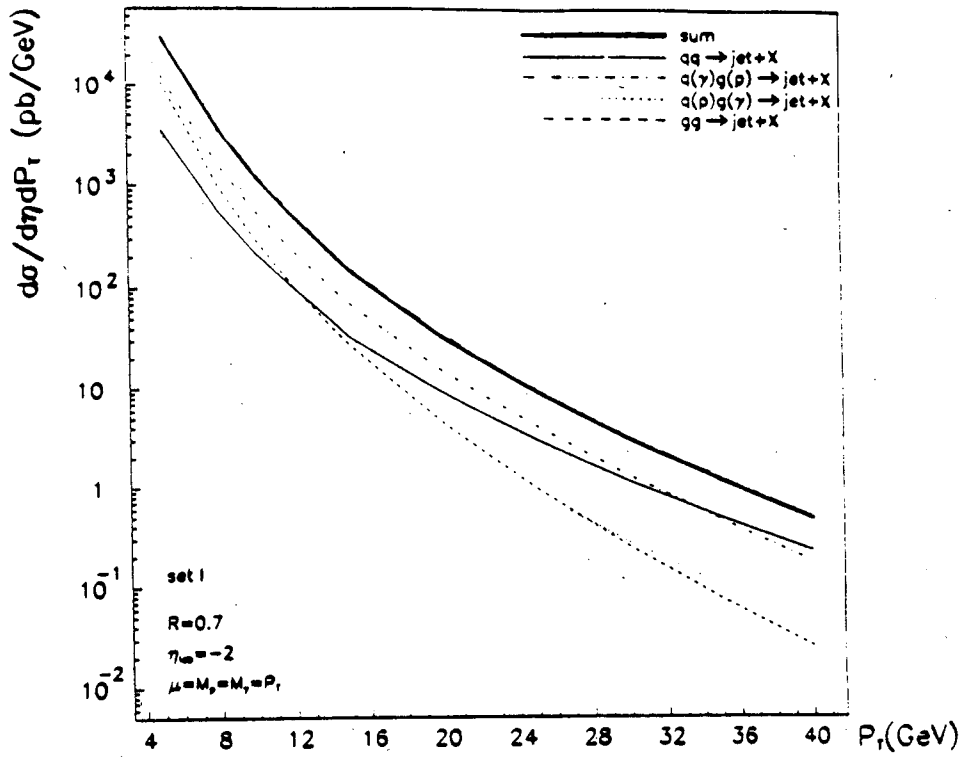

FIG. 4 – p_T distribution $\frac{d\sigma^{(ep)}}{d\eta\, dp_T}\,\eta_{lab} = -2$, R = 0.7, $\mu = M_p = M_\gamma = p_T$. Set I has been used for the photon structure functions. The different parton–parton subprocessed are shown.

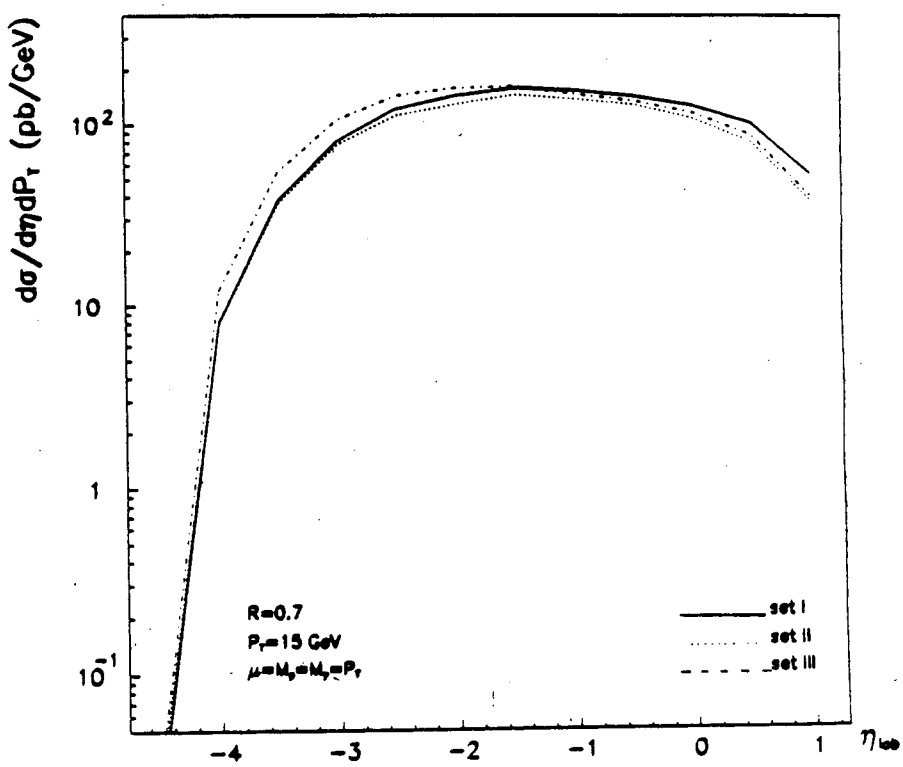

FIG. 5 – η_{lab} distribution $\frac{d\sigma^{(ep)}}{d\eta\, dp_T}$ for p_T = 15 GeV, R = 0.7, $\mu = M_p = M_\gamma = p_T$ and for sets I, II and III of the photon structure functions.

FIGS. 6 – Same as Fig. 5 from the various parton–parton contributions: qq→ jet + X (Fig. 6a); q(γ)g(p) → jet + X (Fig. 6b); q(p)g(γ) → jet + X (Fig. 6c); and gg→ jet + X (Fig. 6d).

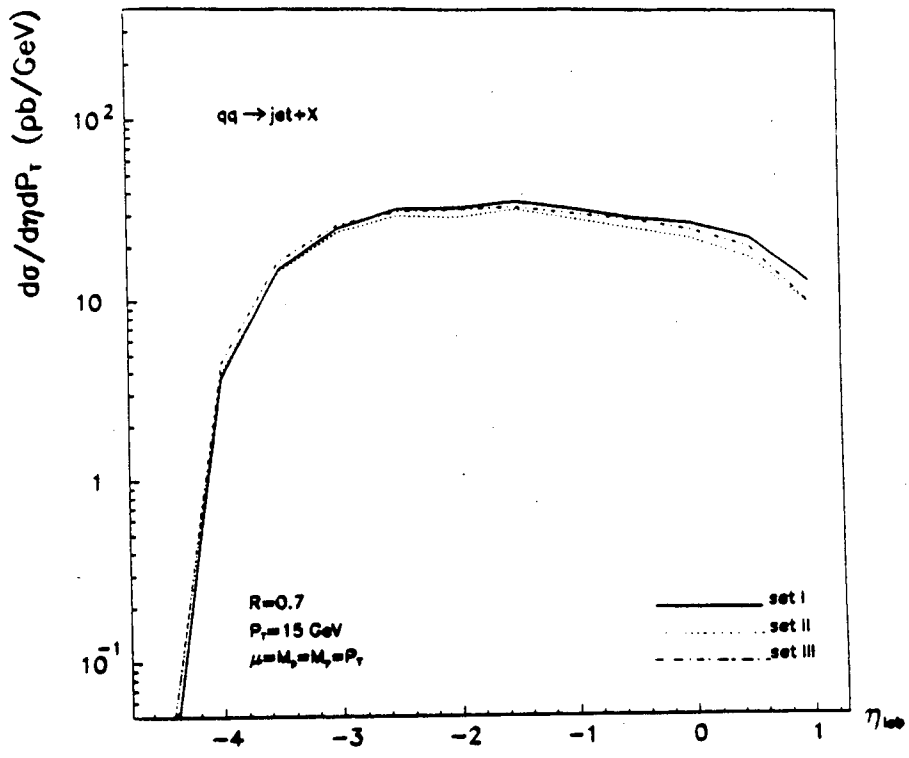

FIG. 6a

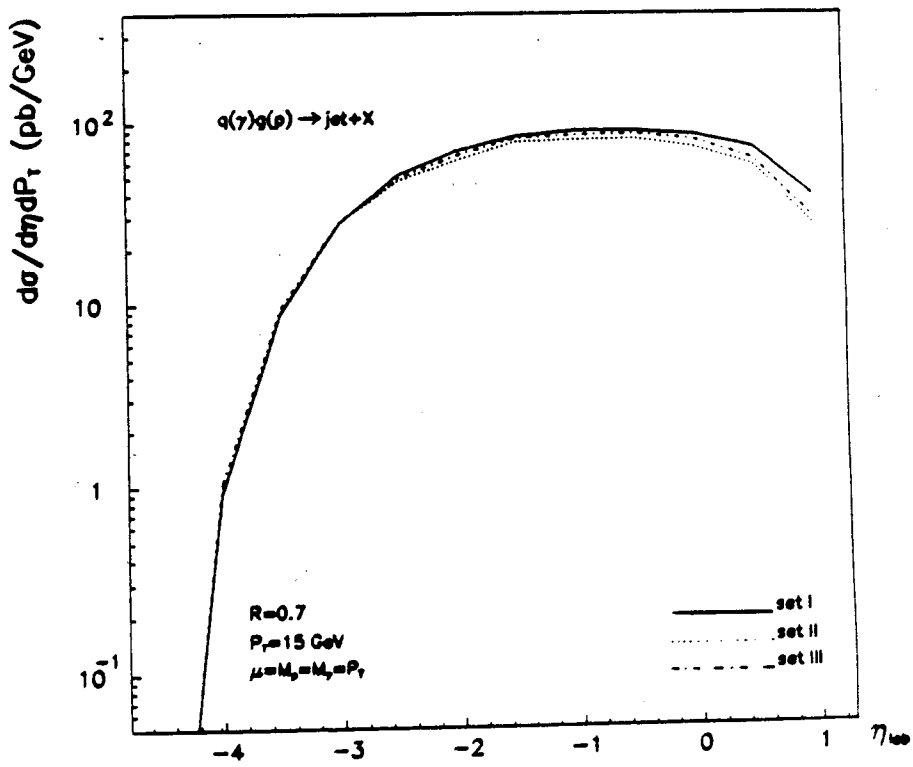

FIG. 6b

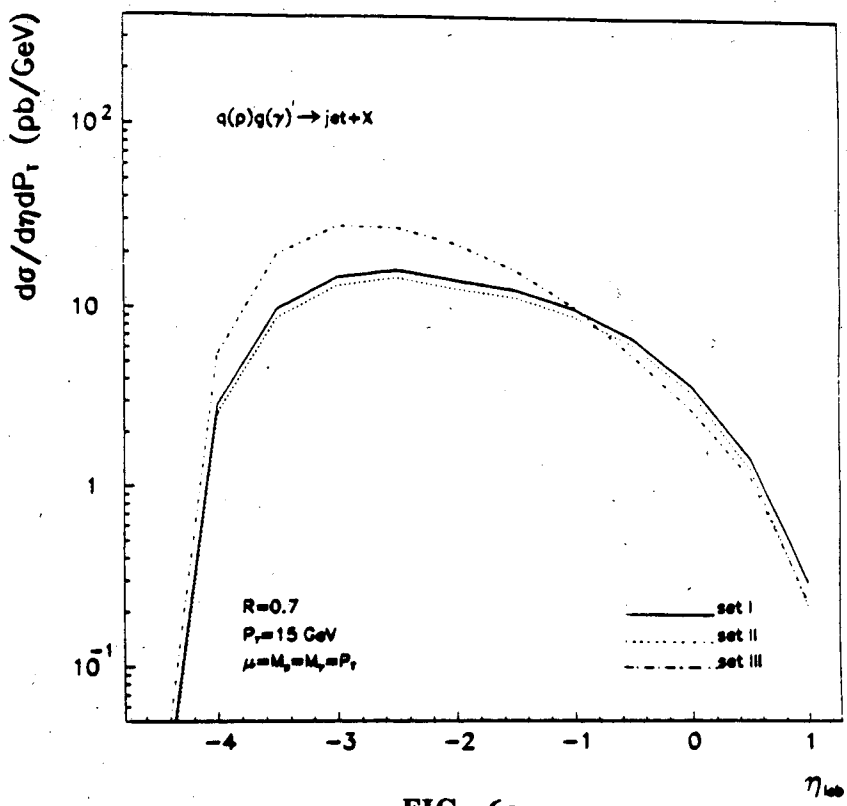
q(p)q(γ) → jet+X
R=0.7
P_T=15 GeV
μ=M_b=M_γ=P_T
set I
set II
set III
dσ/dηdP_T (pb/GeV)
η_lab

FIG. 6c

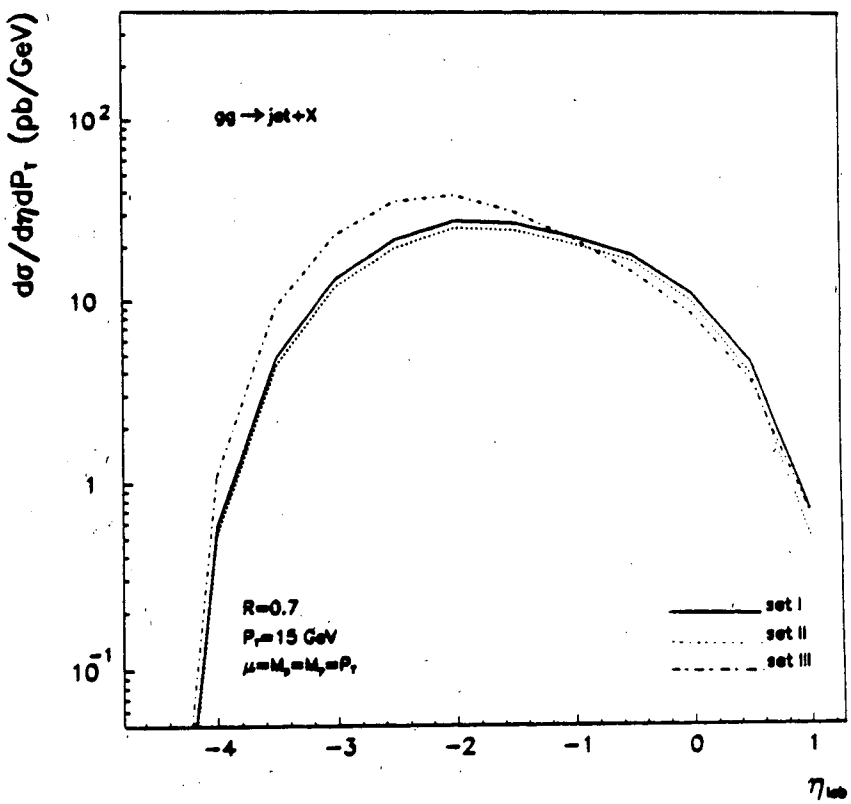
gg → jet+X
R=0.7
P_T=15 GeV
μ=M_b=M_γ=P_T
set I
set II
set III
dσ/dηdP_T (pb/GeV)
η_lab

FIG. 6d

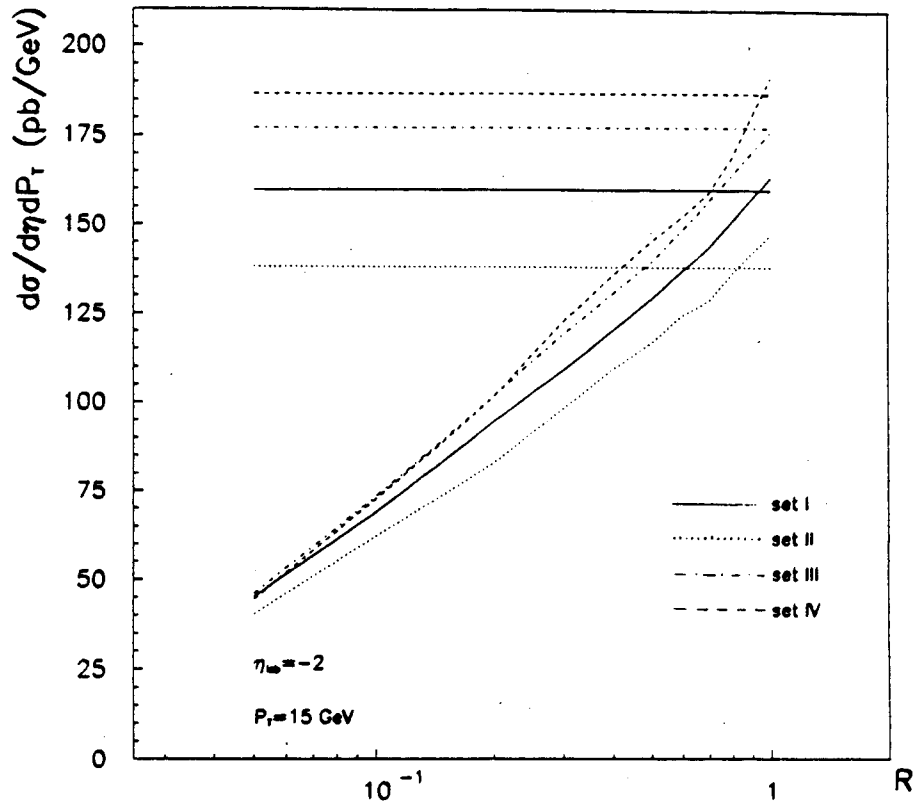

FIG. 7 – Cone size dependence of $\frac{d\sigma^{(ep)}}{d\eta\, dp_T}\,\eta_{lab} = -2$, $p_T = 15$ GeV, $\mu = M_p = M_\gamma = p_T$. Different sets of photon structure functions are compared. The horizontal lines show the Born cross section.

FIGS. 8 – p_T distribution $\frac{d\sigma^{(ep)}}{dp_T}$ for R = 0.7, $\mu = M_p = M_\gamma = p_T$. Different sets of photon structure functions are compared. Various cuts in the pseudorapidity range have been applied: full rang $|\eta_{lab}|$ (Fig. 8a); $|\eta_{lab}| \geq 2.5$ (Fig. 8b); $|\eta_{lab}| \leq 1.5$ (Fig. 8c).

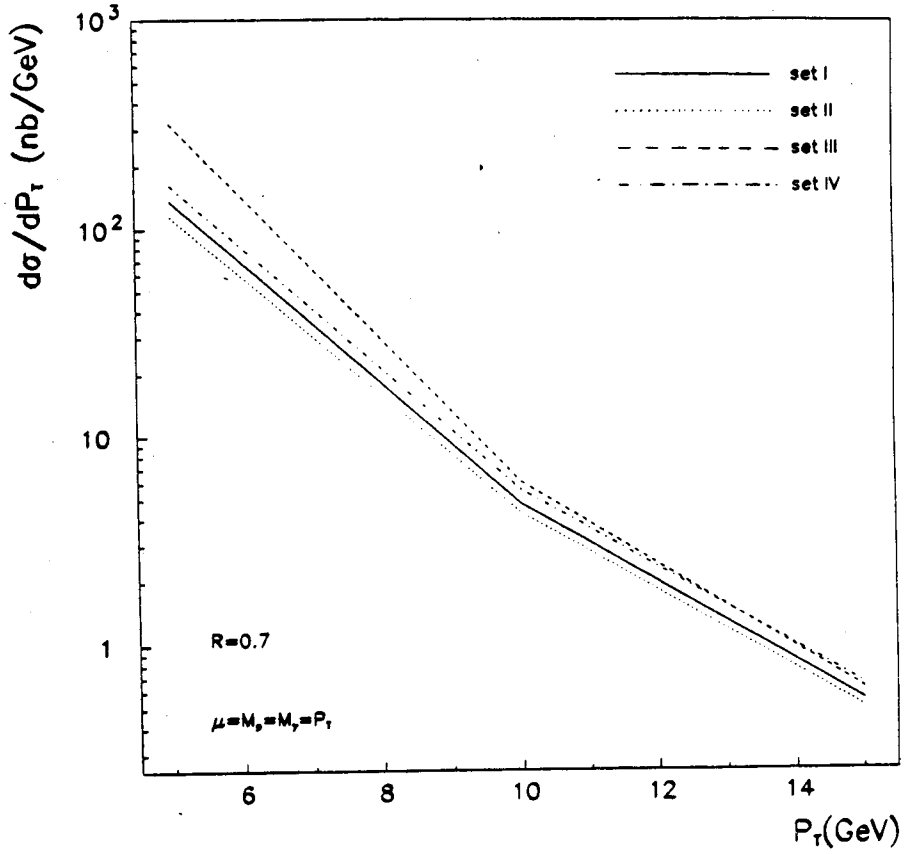

FIG. 8a

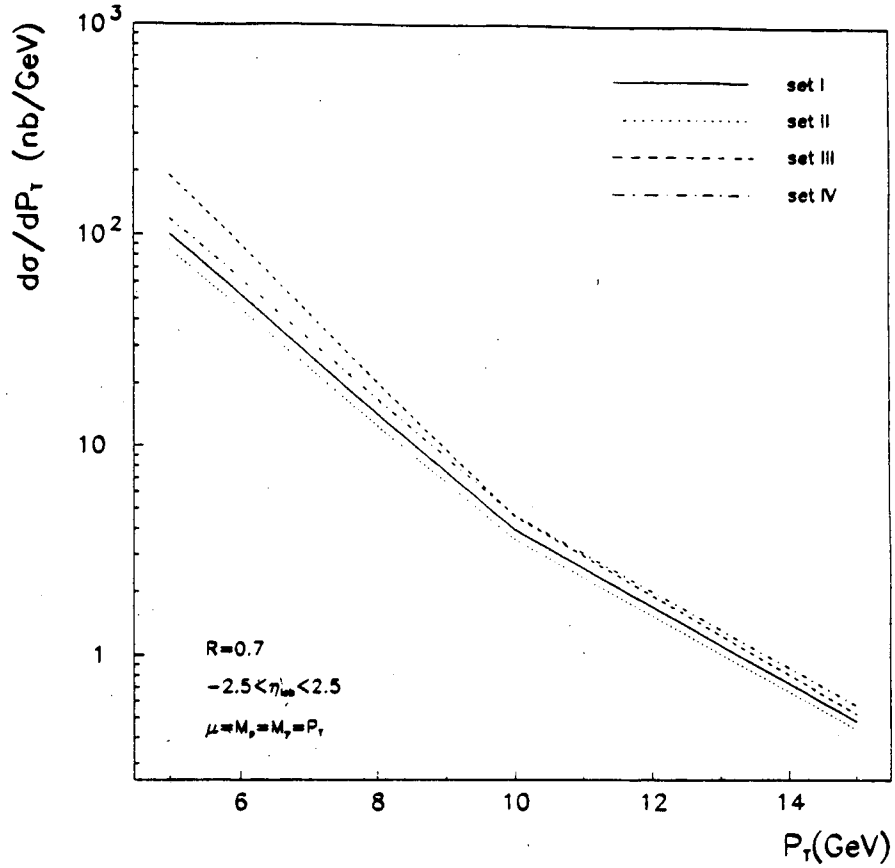
10^3
10^2
10
1
$d\sigma/dP_T$ (nb/GeV)
set I
set II
set III
set IV
R=0.7
$-2.5<\eta_{jet}<2.5$
$\mu=M_p=M_T=P_T$
6
8
10
12
14
P_T(GeV)

FIG. 8b

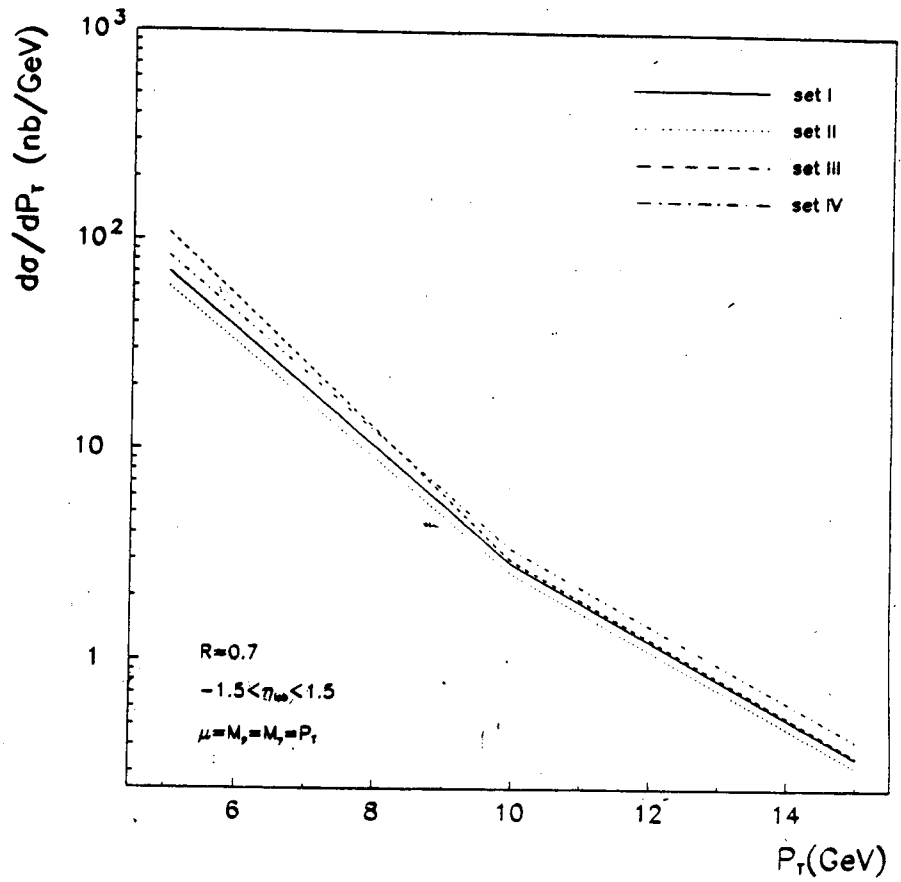
10^3
10^2
10
1
$d\sigma/dP_T$ (nb/GeV)
set I
set II
set III
set IV
R=0.7
$-1.5<\eta_{jet}<1.5$
$\mu=M_p=M_T=P_T$
6
8
10
12
14
P_T(GeV)

FIG. 8c